

## Explosive Synchronization Transitions in Scale-Free Networks

Jesús Gómez-Gardeñes,<sup>1,2,\*</sup> Sergio Gómez,<sup>3</sup> Alex Arenas,<sup>2,3</sup> and Yamir Moreno<sup>2,4</sup>

<sup>1</sup>*Departamento de Física de la Materia Condensada, Universidad de Zaragoza, Zaragoza E-50009, Spain*

<sup>2</sup>*Institute for Biocomputation and Physics of Complex Systems (BIFI), University of Zaragoza, Zaragoza 50009, Spain*

<sup>3</sup>*Departament d'Enginyeria Informàtica i Matemàtiques, Universitat Rovira i Virgili, 43007 Tarragona, Spain*

<sup>4</sup>*Departamento de Física Teórica, Facultad de Ciencias, Universidad de Zaragoza, Zaragoza 50009, Spain*

(Received 30 December 2010; published 23 March 2011)

Explosive collective phenomena have attracted much attention since the discovery of an explosive percolation transition. In this Letter, we demonstrate how an explosive transition shows up in the synchronization of scale-free networks by incorporating a microscopic correlation between the structural and the dynamical properties of the system. The characteristics of the explosive transition are analytically studied in a star graph reproducing the results obtained in synthetic networks. Our findings represent the first abrupt synchronization transition in complex networks and provide a deeper understanding of the microscopic roots of explosive critical phenomena.

DOI: 10.1103/PhysRevLett.106.128701

PACS numbers: 89.75.Hc, 89.20.-a, 89.75.Kd

Synchronization is one of the central phenomena representing the emergence of collective behavior in natural and synthetic complex systems [1–3]. Synchronization processes describe the coherent dynamics of a large ensemble of interconnected dynamical units, such as neurons, fireflies or cardiac pacemakers. The seminal works of Watts and Strogatz [4,5] pointed out the importance of the structure of interactions between units in the emergence of synchronization, which gave rise to the modern framework of complex networks [6]. Since then, the phase transition towards synchronization has been widely studied by considering nontrivial networked interaction patterns [7]. Recent results have shown that the topological features of such networks strongly influence both the value of the critical coupling,  $\lambda_c$ , for the onset of synchronization [8–12] and the stability of the fully synchronized state [13–16]. The case of scale-free (SF) networks has deserved special attention as they are ubiquitously found to represent the backbone of many complex systems. However, the topological properties of the underlying network do not appear to affect the order of the synchronization phase transition, whose second-order nature remains unaltered [8].

More recently, the study of explosive phase transitions in complex networks has attracted a lot of attention since the discovery of an abrupt percolation transition in random [17] and SF networks [18,19]. However, several questions about the microscopic mechanisms responsible of such an explosive transition and their possible existence in other contexts remain open. In this line, we conjecture that dynamical abrupt changes occur when the local heterogeneous structure of networks and the dynamics on top of it, are positively correlated. In this Letter, we prove our conjecture in the context of the synchronization of Kuramoto oscillators. We show that explosive synchronization emerges in SF networks when the natural frequencies of

the oscillators are positively correlated with their degrees. Furthermore, we analytically study this first-order transition in a star graph and show that the combination of heterogeneity and the above correlation is at the core of the explosive transition.

Let us consider an unweighted and undirected network of  $N$  coupled phase oscillators. The phase of each oscillator, denoted by  $\theta_i(t)$  ( $i = 1, \dots, N$ ), evolves in time according to the Kuramoto model [20]:

$$\dot{\theta}_i = \omega_i + \lambda \sum_{j=1}^N A_{ij} \sin(\theta_j - \theta_i), \quad \text{with } i = 1, \dots, N, \quad (1)$$

where  $\omega_i$  stands for the natural frequency of oscillator  $i$ . The connections among oscillators are encoded in the adjacency matrix of the network,  $\mathbf{A}$ , so that  $A_{ij} = 1$  when oscillators  $i$  and  $j$  are connected while  $A_{ij} = 0$  otherwise. Finally, the parameter  $\lambda$  accounts for the strength of the coupling among interconnected nodes.

The original Kuramoto model assumed that the oscillators were connected all-to-all, i.e.  $A_{ij} = 1 \forall i \neq j$ . In this setting, a synchronized state, i.e., a state in which  $\dot{\theta}_i(t) = \dot{\theta}_j(t) \forall i, j$  and  $\forall t$ , shows up when the strength of the coupling  $\lambda$  is larger than a critical value [20–22]. To monitor the transition as  $\lambda$  grows, one quantifies the degree of synchronization among the  $N$  oscillators through [23]

$$r(t)e^{i\Psi(t)} = \frac{1}{N} \sum_{j=1}^N e^{i\theta_j(t)}. \quad (2)$$

The modulus of the above order parameter,  $r(t) \in [0, 1]$ , measures the coherence of the collective motion, reaching the value  $r = 1$  when the system is fully synchronized, while  $r = 0$  for the incoherent solution. On the other hand, the value of  $\Psi(t)$  accounts for the average phase of the collective dynamics of the system. Typically, the average (over long enough times) value of  $r$  as a function of  $\lambda$

displays a second-order phase transition from  $r = 0$  to  $r = 1$  with a critical coupling  $\lambda_c = 2/(\pi g(\omega = 0))$ , where  $g(\omega)$  is the distribution of the natural frequencies,  $\{\omega_i\}$ , and it is assumed to be unimodal and even [23].

Here we will focus on the influence of the dynamical and topological characteristics at the local level in the emergence of global synchronization. In particular, we will identify the internal frequency of each node  $i$  directly with its degree  $k_i$ , so that  $\omega_i = k_i$  in Eq. (1). Note that this prescription sets that  $g(\omega) = P(k)$  but not vice versa [24]. To study the effects of the correlation between dynamical and structural attributes, we simulate the Kuramoto model on top of a family of networks generated according to [25]. This model allows us to construct networks with the same average connectivity,  $\langle k \rangle$ , interpolating from Erdős-Rényi (ER) graphs to Barabási-Albert (BA) SF networks by tuning a single parameter  $\alpha \in [0, 1]$ . For  $\alpha = 1$  one gets ER graphs with a Poissonian degree distribution whereas for  $\alpha = 0$  the resulting networks are SF with  $P(k) \sim k^{-3}$ . Intermediate values of  $\alpha \in (0, 1)$  tune the heterogeneity of the network, which increases when going from  $\alpha = 1$  to  $\alpha = 0$ . In the four panels of Fig. 1, we report the synchronization diagrams of four network topologies constructed using this model. The limiting cases of ER and BA networks correspond to panels 1(a) and 1(d), respectively. The size of these networks is  $N = 10^3$  while  $\langle k \rangle = 6$ .

For each panel in Fig. 1 we have computed two synchronization diagrams,  $r(\lambda)$ , labeled as *forward* and *backward* continuations. The former diagram is computed by increasing progressively the value of  $\lambda$  and computing the stationary value of the order parameter  $r$  for  $\lambda_0, \lambda_0 + \delta\lambda, \dots, \lambda_0 + n\delta\lambda$ . Alternatively, the backward

continuation is performed by decreasing the values of  $\lambda$  from  $\lambda_0 + n\delta\lambda$  to  $\lambda_0$ . The panels 1(a)–1(c) show a typical second-order transition with a perfect match between the backward and forward synchronization diagrams.

The most striking result is however observed for the BA network [panel 1(d)] in which a sharp, first-order synchronization transition appears. In the case of the forward continuation diagram the order parameter remains  $r \approx 0$  until the onset of synchronization in which  $r$  jumps suddenly to  $r \approx 1$  pointing out that almost all the network has reached the synchronous motion. Moreover, the diagram corresponding to the backward continuation also shows a sharp transition from the fully synchronized state to the incoherent one. The two sharp transitions takes place at different values of  $r$  so that the whole synchronization diagram displays a strong hysteresis.

To analyze deeply the change of the order of the synchronization transition, we have computed the effective frequency along the forward continuation (see Fig. 2) as

$$\omega_i^{\text{eff}} = \frac{1}{T} \int_t^{t+T} \dot{\theta}_i(\tau) d\tau, \quad (3)$$

with  $T \gg 1$ . In addition, we have computed the evolution of  $\omega_i^{\text{eff}}$  within a degree class  $k$ ,  $\langle \omega \rangle_k$ , by averaging over the  $N_k = NP(k)$  nodes that have identical degree  $k$ , i.e.,  $\langle \omega \rangle_k = \sum_{[i|k_i=k]} \omega_i^{\text{eff}} / N_k$ . From the panels in Fig. 2 we observe that the individual frequencies and the different curves  $\langle \omega \rangle_k(\lambda)$  converge progressively to the average frequency of the system  $\Omega = \langle k \rangle = 6$  until full synchronization is achieved. Panel 2(a) (ER graph) shows that the convergence to  $\Omega$  is first achieved by those nodes with large degree while the small  $k$  classes achieve full synchronization later on. As the heterogeneity of the network increases [see  $\alpha = 0.6$  and  $\alpha = 0.2$  in panels 2(b) and 2(c), respectively] the differences in the convergence of the  $k$  classes decrease. Finally, for the BA network [Fig. 2(d)], the nodes (and thus the different  $k$  classes) retain their natural frequencies until they become locked, which signals the abrupt synchronization observed in Fig. 1(d). Thus, the first-order transition of the BA network corresponds to a process in which no microscopic signals of synchronization are observed until  $\lambda_c$  is reached.

To further explore the correspondence of the explosive synchronization transition with the SF nature of the underlying graph, in Fig. 3(a) we show the synchronization diagrams for different uncorrelated SF graphs with different degree-distribution' exponents. These graphs have been constructed using the configurational model [26] by imposing a degree distribution  $P(k) \sim k^{-\gamma}$  with  $\gamma = 2.4, 2.7, 3.0,$  and  $3.3$ . The synchronization diagrams are obtained by forward continuation (as described above) starting at  $\lambda = 1$  and performing adiabatic increments of  $\delta\lambda = 0.02$ . Again, for each value of  $\lambda$  the Kuramoto dynamics is run until the value of  $r$  reaches its stationary state. From the figure it is clear that a first-order

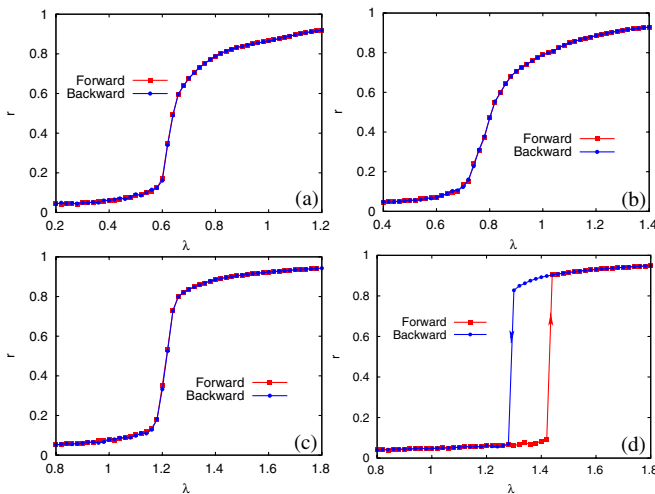


FIG. 1 (color online). Synchronization diagrams  $r(\lambda)$  for different networks constructed using the model in [25]. The  $\alpha$  values in each panel are (a)  $\alpha = 1$  (ER), (b)  $\alpha = 0.6$ , (c)  $\alpha = 0.2$  and (d)  $\alpha = 0$  (BA). The panels show both forward and backward continuations in  $\lambda$  using  $\delta\lambda = 0.02$ . The size of the networks is  $N = 10^3$  and  $\langle k \rangle = 6$ .

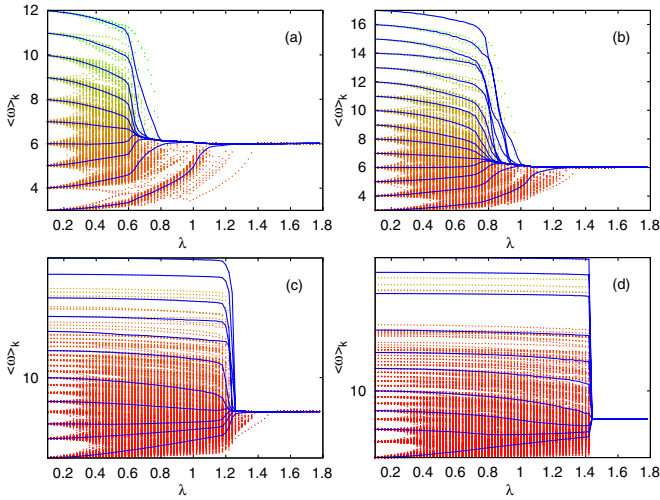


FIG. 2 (color online). The panels show the evolution of the effective frequencies of the nodes along the (forward) continuation in the model networks of Fig. 1. The colored dots account for single-node values (colors stand for their respective degree) while solid lines show the average value of the effective frequencies of nodes having the same degree.

synchronization transition appears for all the reported values of  $\gamma$  pointing out the ubiquity of the explosive synchronization transition in SF networks. Moreover, the onset of synchronization,  $\lambda_c$ , is delayed as  $\gamma$  decreases.

Up to now, we have shown that the explosive synchronization transition appears in SF when the natural frequencies of the nodes are correlated with their degrees. To show that this correlation is the responsible of such explosive transition, in Fig. 3(b) we show the synchronization diagram for the same SF networks used in Fig. 3(a), but when the correlation between dynamics and structure is broken in such a way that the same distribution for the internal frequencies,  $g(\omega) = \omega^{-\gamma}$  is kept. To this end, we made a random assignment of frequencies to nodes according to  $g(\omega)$ . The plots reveal that now all the transitions turn to be of second order, thus recovering the usual picture of synchronization phenomena in complex networks. Therefore, the first-order transition arises due to the positive correlation between natural frequencies and the degrees of the nodes in SF networks [27].

To get analytical insights, we reduce the problem studied to the analysis of the *star* configuration, a special structure that grasp the main property of SF networks, namely, the role of hubs. Therefore, we explore the synchronization transition of such a configuration and show that it is indeed explosive when the correlation  $\omega_i = k_i$  holds. A star graph [as shown in the inset of Fig. 4(a)] is composed by a central node (the hub) and  $K$  peripheral nodes (or leaves). Each of the peripheral nodes connects solely to the hub. Thus, the connectivity of the leaves is  $k_i = 1$  ( $i = 1, \dots, K$ ) while that of the hub is  $k_h = K$ . Let us suppose that the hub has a frequency  $\omega_h$  while all the leaves beat at the same frequency  $\omega$ .

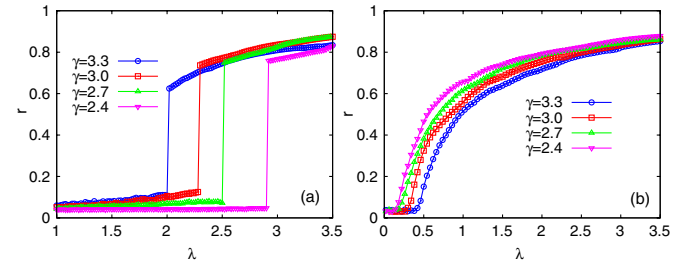


FIG. 3 (color online). Panel (a) shows the synchronization diagrams  $r(\lambda)$  for several SF networks constructed via the configurational model. All the networks have a degree distribution  $P(k) \sim k^{-\gamma}$  with  $\gamma = 2.4, 2.7, 3.0$ , and  $3.3$  while  $N = 10^3$ . The steps of the continuation are set to  $\delta\lambda = 0.02$ . In panel (b) we show the synchronization diagrams of the same SF networks without the local correlation between degrees and natural frequencies, i.e.,  $\omega_i \neq k_i$ , while  $g(\omega) \sim \omega^{-\gamma}$ .

First we set a reference frame rotating with the average phase of the system,  $\Psi(t) = \Psi(0) + \Omega t$ , being  $\Omega$  the average frequency of the oscillators in the star,  $\Omega = (K\omega + \omega_h)/(K + 1)$ . In the following we set  $\Psi(0) = 0$  without loss of generality so that the transformed variables are defined as  $\phi_h = \theta_h - \Omega t$  for the hub and  $\phi_j = \theta_j - \Omega t$  (with  $j = 1, \dots, K$ ) for the leaves. Thus, the equations of motion for the hub and the leaves read

$$\dot{\phi}_h = (\omega_h - \Omega) + \lambda \sum_{j=1}^K \sin(\phi_j - \phi_h), \quad (4)$$

$$\dot{\phi}_j = (\omega - \Omega) + \lambda \sin(\phi_h - \phi_j), \quad \text{with } j = 1 \dots K. \quad (5)$$

In this rotating frame Eq. (4) can be expressed as

$$\dot{\phi}_h = (\omega_h - \Omega) + \lambda(K + 1)r \sin(\phi_h); \quad (6)$$

note that in this new frame it is easy to identify that the dynamics of the hub is governed by its new inherent frequency and the superposition of a set of identical signals from the leaves. Now, imposing that the phase of the hub is locked,  $\dot{\phi}_h = 0$ , we obtain

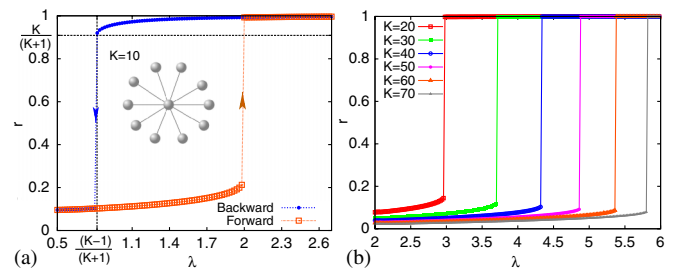


FIG. 4 (color online). Synchronization diagrams for the star graph [see the inset in plot (a)]. In (a) we show the (forward and backward) continuation diagrams for  $K = 10$  while (b) shows the forward continuation diagrams for star graphs of different sizes as indicated.



$$\sin\phi_h = \frac{(\omega_h - \Omega)}{\lambda(K+1)r}. \quad (7)$$

Now we consider the equations for the leaves, Eq. (5), and evaluate the expression for  $\cos\phi_j$  in the locked regime,  $\dot{\phi}_j = 0$ . After some algebra, we get

$$\cos\phi_j = \frac{(\Omega - \omega)\sin\phi_h \pm \sqrt{[1 - \sin^2\phi_h][\lambda^2 - (\Omega - \omega)^2]}}{\lambda}. \quad (8)$$

The above expression is valid only when  $(\Omega - \omega) \leq \lambda$ . From this inequality we obtain the value of the coupling  $\lambda$  for which the phase-locking is lost, i.e., the critical coupling  $\lambda_c = \Omega - \omega$ . In our case, we have  $\omega_h = K$ ,  $\omega = 1$  and  $\Omega = 2K/(K+1)$  so that we obtain a critical coupling  $\lambda_c = (K-1)/(K+1)$ . On the other hand, we can derive the value  $r_c$  of the order parameter at the critical point by using Eq. (7) and (8) to compute  $r = \langle \cos(\phi) \rangle$  at  $\lambda_c$ :

$$r_c = \left. \frac{\cos(\phi_h) + K \cos(\phi_j)}{K+1} \right|_{\lambda_c} = \frac{K}{(K+1)}. \quad (9)$$

Therefore, as  $r_c > 0$ , when the synchronization is lost there is a gap in the synchronization diagram pointing out the existence of a first-order synchronization transition. Moreover, as  $K$  increases both  $\lambda_c$  and  $r_c$  tend to 1 thus confirming the first-order nature of the transition in the thermodynamic limit,  $K \rightarrow \infty$ . As shown in Fig. 4(a) for the case  $K = 10$ , the theoretical values of  $\lambda_c$  and  $r_c$ , are in perfect agreement with results from numerical simulations. Finally, as shown in Fig. 4(b), the stability of the unlocked phase regime,  $r \approx 0$ , increases with  $K$  so that we can reach larger values of  $\lambda$  by continuing (forward) the solution with  $r \approx 0$ . As a result, the hysteresis cycle grow with  $K$ .

Summing up, we have shown that an explosive synchronization transition occurs in SF networks when there is a positive correlation between the structural (the degrees) and dynamical (natural frequencies) properties of the nodes. This constitutes the first example of an explosive synchronization transition in complex networks. Moreover, we have shown that the emergence of such transition is intrinsically due to the interplay between the local structure and the internal dynamics of nodes rather than being caused by any particular form of the distribution of natural frequencies. Our findings provide with an explosive phase transition of an important macroscopic phenomena, synchronization, in a widely studied dynamical framework, the Kuramoto model, thus shedding light to the microscopic roots behind these phenomena and paving the way to their study in other dynamical contexts.

Work supported by Spanish MICINN Ramón y Cajal (J.G.-G), FIS2008-01240, MTM2009-13848, FIS2009-13364-C02-01, FIS2009-13730-C02-02, and Generalitat de Catalunya 2009-SGR-838.

\*gardenes@gmail.com

- [1] A. T. Winfree, *The Geometry of Biological Time* (Springer-Verlag, New York, 1990).
- [2] S. H. Strogatz, *Sync: The Emerging Science of Spontaneous Order* (Hyperion, New York, 2003).
- [3] A. Pikovsky, M. Rosenblum, and J. Kurths, *Synchronization: A Universal Concept in Nonlinear Sciences* (Cambridge University Press, Cambridge, England, 2003).
- [4] D. J. Watts and S. H. Strogatz, *Nature (London)* **393**, 440 (1998).
- [5] S. H. Strogatz, *Nature (London)* **410**, 268 (2001).
- [6] S. Boccaletti *et al.*, *Phys. Rep.* **424**, 175 (2006).
- [7] A. Arenas *et al.*, *Phys. Rep.* **469**, 93 (2008).
- [8] Y. Moreno and A. F. Pacheco, *Europhys. Lett.* **68**, 603 (2004).
- [9] D.-S. Lee, *Phys. Rev. E* **72**, 026208 (2005).
- [10] A. Arenas, A. Díaz-Guilera, and C. J. Perez-Vicente, *Phys. Rev. Lett.* **96**, 114102 (2006).
- [11] C. Zhou and J. Kurths, *Chaos* **16**, 015104 (2006).
- [12] J. Gómez-Gardeñes, Y. Moreno, and A. Arenas, *Phys. Rev. Lett.* **98**, 034101 (2007).
- [13] L. M. Pecora and T. L. Carroll, *Phys. Rev. Lett.* **80**, 2109 (1998).
- [14] M. Barahona and L. M. Pecora, *Phys. Rev. Lett.* **89**, 054101 (2002).
- [15] T. Nishikawa *et al.*, *Phys. Rev. Lett.* **91**, 014101 (2003).
- [16] C. Zhou, A. E. Motter, and J. Kurths, *Phys. Rev. Lett.* **96**, 034101 (2006).
- [17] D. Achlioptas, R. M. D'Souza, and J. Spencer, *Science* **323**, 1453 (2009).
- [18] F. Radicchi and S. Fortunato, *Phys. Rev. Lett.* **103**, 168701 (2009).
- [19] Y. S. Cho *et al.*, *Phys. Rev. Lett.* **103**, 135702 (2009).
- [20] Y. Kuramoto, *Lect. Notes Phys.* **39**, 420 (1975).
- [21] Y. Kuramoto, *Chemical Oscillations, Waves, and Turbulence* (Springer-Verlag, New York, 1984).
- [22] J. A. Acebron *et al.*, *Rev. Mod. Phys.* **77**, 137 (2005).
- [23] S. H. Strogatz, *Physica D (Amsterdam)* **143**, 1 (2000).
- [24] Our main results hold when  $w_i \sim k_i^\alpha$  with  $\alpha > 0$ , i.e., when  $w_i$  is positively correlated with  $k_i$ .
- [25] J. Gómez-Gardeñes and Y. Moreno, *Phys. Rev. E* **73**, 056124 (2006).
- [26] M. Molloy and B. Reed, *Random Struct. Algorithms* **6**, 161 (1995).
- [27] We have obtained synchronization diagrams for several degree-frequency correlations. To this end, we initially assign  $\omega_i = k_i$  with probability  $(1-p)$  while, with probability  $p$ ,  $\omega_i$  is randomly drawn from a distribution  $P(\omega) \sim \omega^{-\gamma}$ . In a supplemental figure [28] we show the diagrams  $r(\lambda)$  for different values of  $p$  in a SF network with  $\gamma = 2.4$ . It is shown that for  $p > 0$  explosive synchronization remains while at some value  $p_c < 1$  the transition turns into a second-order one.
- [28] See supplemental material at <http://link.aps.org/supplemental/10.1103/PhysRevLett.106.128701>.



Supplemental material

# Explosive Synchronization Transitions in Scale-free Networks

Jesús Gómez-Gardeñes, Sergio Gómez, Alex Arenas, and Yamir Moreno

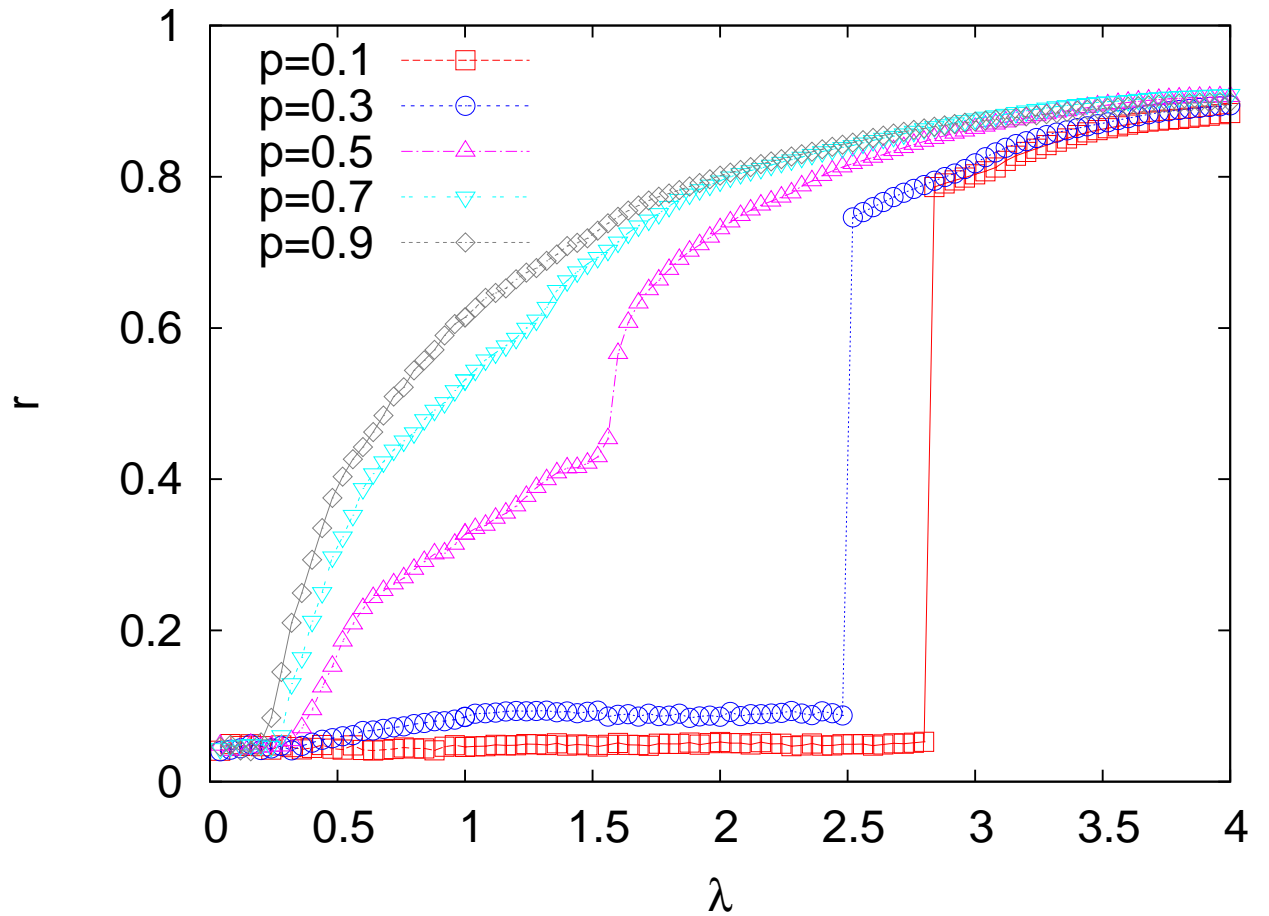


Figure 1: This supplementary figure shows the synchronization diagrams of a scale-free network with degree distribution  $P(k) \sim k^{-2.4}$  when an intermediate degree-frequency correlation is initially set as described in the footnote (reference [27]). In particular, the figure shows the diagrams for the cases  $p = 0.1, 0.3, 0.5, 0.7, 0.9$  of the frequency assignment process described in [27].